Preprint Title	1,2,5-Oxadiazole-1,2,3,4-Tetrazole Based High Energy Materials: Molecule Design and Screen
Authors	Xinghui Jin, Menghui Xiao, Jianhua Zhou and Bingcheng Hu
Publication Date	13 Jul 2020
Article Type	Full Research Paper
Supporting Information File 1	Supporting Information.doc; 249.5 KB
ORCID® iDs	Xinghui Jin - https://orcid.org/0000-0001-9392-8964

1,2,5-Oxadiazole-1,2,3,4-Tetrazole Based High Energy Materials: Molecule Design and Screen

Xinghui Jin*[a], Menghui Xiao,[a] Jianhua Zhou,[a] Bingcheng Hu[b]
[a]Key Laboratory of Fine Chemicals in Universities of Shandong, School of Chemistry and Pharmaceutical Engineering, Qilu University of Technology (Shandong Academy of Sciences), Ji'nan 250353, China
[b]School of Chemical Engineering, Nanjing University of Science and Technology, Nanjing, 210094, China
*For Correspondence, Email: jingetiema0000@126.com

Abstract: A series of 1,2,5-oxadiazole-1,2,3,4-tetrazole based high energy materials were theoretically designed and investigated. Their heats of formation, detonation properties and thermal stabilities were calculated by isodesmic reactions, Kamlet-Jacobs equations and bond dissociation energies, respectively. The results show that all the designed compounds possess high positive heats of formation and the –N=N–/–N_3 substituents were found to be more helpful in improving the heats of formation than other substituents. The change tendency of densities, detonation pressures and detonation velocities were approximately the same to each other which suggests that values of densities were the key parameter to detonation properties rather than other parameters. In view of bond dissociation energies, the –CN/–NH_2 substituents will be helpful to improve the thermal stabilities of the designed compounds while the other substituents/bridges will decrease their thermal stabilities to some extent. Take detonation properties and thermal stabilities into consideration, six compounds (C7, D3, D7, F7, G7 and H7) were selected as potential high energy density compounds since they had higher detonation properties and thermal stabilities than those of RDX. Finally, electronic structures (such as distribution of frontier molecular orbitals and electrostatic potentials) of the selected compounds were simulated to give a better understanding of these compounds.

Key words: 1,2,5-Oxadiazole, 1,2,3,4-Tetrazole, High energy materials, Energetic properties, Thermal stabilities

1. Introduction

In the last few decades, explosives and propellants as a special type of energy materials have been widely used both in military and civilian.[1-4] High energy materials with excellent detonation properties (contain detonation velocity (*D*) and detonation pressure (*P*)) and acceptable thermal stabilities were always acted as the ultimate goal for the researcher in this filed.[5-8] In most case, researchers were interested in developing new high energy materials based on five/six-membered nitrogen rich rings since these moieties often possess high positive heats of formation (HOF).[9,10] Except for high positive heats of formation, oxygen balance (OB) was also an important parameter to be considered when an energetic molecule was designed. This is because OB was an index that indicates the degree to which an explosive can be oxidized.[11,12] Generally speaking, oxygen atoms in $C_aH_bO_cN_d$ compound required to convert all the carbon atoms into CO_2 while all the hydrogen atoms into H_2O and thus, OB values which were near to zero will have more improved energetic properties. Not surprisingly, oxadiazoles were this type of structures containing a large amount of C-N/N-N energetic bonds and oxygen atoms and thus, makes it attract considerable attention during the process of discovering novel high energy materials. Usually, there exists four oxadiazole isomers which were named as 1,2,4-oxadiazole, 1,2,5-oxadiazole, 1,3,4-oxadiazole, and 1,2,3-oxadiazole. Among these isomers, 1,2,5-oxadiazole (furazan) had the highest positive heats of formation and a large number of energetic group-functionalized monofurazan/macrocyclic/linked/ring-fused furazans were designed and synthesized.[13-15] However, furazan ring is very sensitive and the efforts to discovery new high energy materials with maximize detonation properties and minimizing sensitivity were still on the way. Previous research have also demonstrated that the π-π conjugate system has the potential to reduce sensitivities and increase detonation properties consequently, 1,2,3,4-tetrazole, which also possesses high positive heats of formation and π-π conjugate system, was considered to form different high energy materials.[16]

In this work, a series of 1,2,5-oxadiazole-1,2,3,4-tetrazole based high energy materials were designed and investigated by density functional theory (DFT)[17-20] at B3LYP/6-311G(d,p) level. (Scheme 1) Their heats of formation, detonation properties and thermal stabilities were predicted by designing isodesmic reactions, Kamlet-Jacobs equations and bond dissociation energies (BDE), respectively (all the detailed computational information can be found in the Supporting Information). Finally, potential high energy materials with excellent detonation properties and acceptable thermal stabilities were screened and their physicochemical properties (such as the distribution of frontier molecular orbital, electrostatic potentials and contour line maps of the electronic densities) were simulated to give a better understanding of these screened compounds.

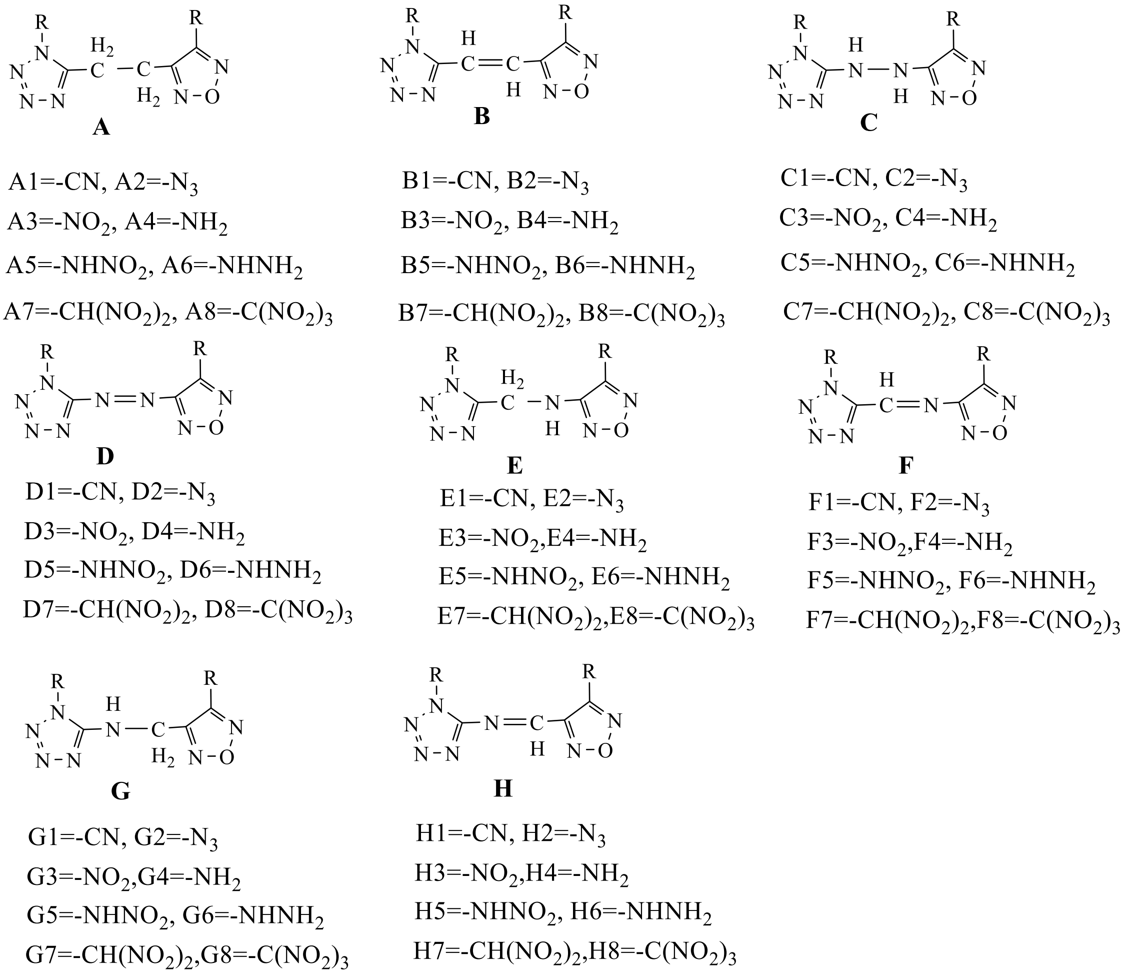

A

A1=-CN, A2=$-N_3$
A3=$-NO_2$, A4=$-NH_2$
A5=$-NHNO_2$, A6=$-NHNH_2$
A7=$-CH(NO_2)_2$, A8=$-C(NO_2)_3$

B

B1=-CN, B2=$-N_3$
B3=$-NO_2$, B4=$-NH_2$
B5=$-NHNO_2$, B6=$-NHNH_2$
B7=$-CH(NO_2)_2$, B8=$-C(NO_2)_3$

C

C1=-CN, C2=$-N_3$
C3=$-NO_2$, C4=$-NH_2$
C5=$-NHNO_2$, C6=$-NHNH_2$
C7=$-CH(NO_2)_2$, C8=$-C(NO_2)_3$

D

D1=-CN, D2=$-N_3$
D3=$-NO_2$, D4=$-NH_2$
D5=$-NHNO_2$, D6=$-NHNH_2$
D7=$-CH(NO_2)_2$, D8=$-C(NO_2)_3$

E

E1=-CN, E2=$-N_3$
E3=$-NO_2$,E4=$-NH_2$
E5=$-NHNO_2$, E6=$-NHNH_2$
E7=$-CH(NO_2)_2$,E8=$-C(NO_2)_3$

F

F1=-CN, F2=$-N_3$
F3=$-NO_2$,F4=$-NH_2$
F5=$-NHNO_2$, F6=$-NHNH_2$
F7=$-CH(NO_2)_2$,F8=$-C(NO_2)_3$

G

G1=-CN, G2=$-N_3$
G3=$-NO_2$,G4=$-NH_2$
G5=$-NHNO_2$, G6=$-NHNH_2$
G7=$-CH(NO_2)_2$,G8=$-C(NO_2)_3$

H

H1=-CN, H2=$-N_3$
H3=$-NO_2$,H4=$-NH_2$
H5=$-NHNO_2$, H6=$-NHNH_2$
H7=$-CH(NO_2)_2$,H8=$-C(NO_2)_3$

Scheme 1. Designed molecules based on 1,2,5-oxadiazole

2. Results and discussion

2.1 Frontier molecular orbital (FMO)

Frontier molecular orbitals (FMOs), which contains the highest occupied molecular orbitals (HOMOs) and the lowest unoccupied molecular orbitals (LUMOs), as well as their energy gap ($\Delta E_{\text{LUMO-HOMO}}$) were important aspects to evaluate the chemical reactivity of molecules with similar skeletons.[21,22] Generally speaking, compounds with high values of $\Delta E_{\text{LUMO-HOMO}}$ will possess lower chemical reactivity. Table 1 presented the E_{HOMO}, E_{LUMO} and $\Delta E_{\text{LUMO-HOMO}}$ of the designed compounds. For a comparison, E_{HOMO}, E_{LUMO} and $\Delta E_{\text{LUMO-HOMO}}$ of the parent structures were also listed in the table. It is seen that E_{HOMO}, E_{LUMO} and $\Delta E_{\mathrm{LUMO\text{-}HOMO}}$ of the substituted compounds were from -9.29 (A8) to -6.21 eV (E6), from -5.19 (D7) to -0.81 eV (E6) and from 3.26 (D6) to 6.10 (A1), respectively. Obviously, compounds E6 had the highest E_{HOMO} and E_{LUMO}, which suggests that the combination of $–NHNH_2$ and $–CH_2NH–$ bridge will increase the values of E_{HOMO} and E_{LUMO}. However, no regularity was found for the minimum values of E_{HOMO}, E_{LUMO}: the fact is that compound with the$–C(NO_2)_3$ group and $–CH_2CH_2–$ bridge will decrease the E_{HOMO} while the combination of $–CH(NO_2)_2$ group and –N=N– bridge will decrease E_{LUMO} apparently. In view of $\Delta E_{\mathrm{LUMO\text{-}HOMO}}$, compound D6 had the lowest $\Delta E_{\mathrm{LUMO\text{-}HOMO}}$ and compound A1 had the highest value. It was predicted that compound D6 will be the most chemical reactive while compound A1will be the most insensitive member under external stimuli or extreme conditions. Interesting results were also found as follows: (1) for E_{HOMO}, compounds substituted by $–NH_2$ and $–NHNH_2$ groups possess higher values of E_{HOMO} for series C, D and G than their parent structures. But for series A, B, E, F and H, the case is that compounds substituted by $–N_3$, $–NH_2$ and $–NHNH_2$ groups possess higher values of E_{HOMO} than their parent structures; (2) for E_{LUMO}: when the parent structures were substituted by $–NH_2$ and $–NHNH_2$ groups, values of t E_{LUMO} were higher than their parent structures except for series C and D; (3) for $\Delta E_{\mathrm{LUMO\text{-}HOMO}}$: compounds have lower values of $\Delta E_{\mathrm{LUMO\text{-}HOMO}}$ than their parent structures for series B, C, D, F and H. It can be predicted that the addition of energetic groups to the parent structures will decrease the stabilities of all the designed compounds except for compounds A1, E4 and G1. Overall, compounds with different parent structures and energetic groups possess different E_{HOMO}, E_{LUMO} and $\Delta E_{\mathrm{LUMO\text{-}HOMO}}$, suggesting that the influence of bridges on E_{HOMO}, E_{LUMO} and $\Delta E_{\mathrm{LUMO\text{-}HOMO}}$ were coupled to those of energetic groups.

Table 1 Calculated E_{HOMO} and E_{LUMO} (eV) and energy gaps ($\Delta E_{\mathrm{LUMO–HOMO}}$) of the designed compounds

Compd.	**A**	**A1**	**A2**	**A3**	**A4**	**A5**	**A6**	**A7**	**A8**
HOMO	-7.83	-9.04	-7.79	-8.97	-7.10	-8.41	-7.10	-8.99	-9.29
LUMO	-2.18	-2.94	-2.73	-3.77	-1.18	-2.89	-1.52	-3.72	-4.34
$\Delta E_{\mathrm{LUMO\text{-}HOMO}}$	5.65	6.10	5.06	5.20	5.92	5.52	5.58	5.27	4.95
Compd.	**B**	**B1**	**B2**	**B3**	**B4**	**B5**	**B6**	**B7**	**B8**
HOMO	-7.48	-8.44	-7.37	-8.29	-6.93	-7.95	-6.94	-8.49	-8.57

LUMO	-2.93	-3.96	-3.08	-4.14	-2.63	-3.47	-2.82	-3.99	-4.32
$\Delta E_{\text{LUMO-HOMO}}$	4.55	4.48	4.29	4.15	4.30	4.48	4.12	4.50	4.25
Compd.	**C**	**C1**	**C2**	**C3**	**C4**	**C5**	**C6**	**C7**	**C8**
HOMO	-7.31	-8.36	-7.33	-8.17	-6.68	-8.01	-7.06	-8.76	-8.36
LUMO	-1.46	-3.01	-2.80	-3.92	-1.17	-3.22	-1.50	-3.99	-4.34
$\Delta E_{\text{LUMO-HOMO}}$	5.85	5.35	4.53	4.25	5.51	4.79	5.56	4.77	4.02
Compd.	**D**	**D1**	**D2**	**D3**	**D4**	**D5**	**D6**	**D7**	**D8**
HOMO	-7.82	-8.77	-7.85	-8.72	-7.24	-8.47	-7.22	-8.97	-8.98
LUMO	-3.83	-4.88	-4.00	-4.80	-3.71	-4.60	-3.96	-5.19	-5.16
$\Delta E_{\text{LUMO-HOMO}}$	3.99	3.89	3.85	3.92	3.53	3.87	3.26	3.78	3.82
Compd.	**E**	**E1**	**E2**	**E3**	**E4**	**E5**	**E6**	**E7**	**E8**
HOMO	-7.52	-8.05	-7.09	-7.91	-6.89	-7.32	-6.21	-8.33	-8.26
LUMO	-1.87	-2.84	-2.77	-3.82	-1.22	-2.80	-0.81	-3.89	-4.26
$\Delta E_{\text{LUMO-HOMO}}$	5.65	5.21	4.32	4.09	5.67	4.52	5.40	4.44	4.00
Compd.	**F**	**F1**	**F2**	**F3**	**F4**	**F5**	**F6**	**F7**	**F8**
HOMO	-8.07	-8.97	-7.55	-8.82	-6.91	-8.29	-6.83	-9.07	-9.14
LUMO	-3.31	-4.36	-3.64	-4.43	-3.07	-3.60	-2.69	-4.41	-4.63
$\Delta E_{\text{LUMO-HOMO}}$	4.76	4.61	3.91	4.39	3.84	4.69	4.14	4.66	4.51
Compd.	**G**	**G1**	**G2**	**G3**	**G4**	**G5**	**G6**	**G7**	**G8**
HOMO	-7.04	-8.16	-7.27	-8.04	-6.83	-7.40	-6.50	-8.33	-8.17
LUMO	-2.40	-3.27	-2.48	-4.08	-1.66	-2.98	-1.39	-3.84	-4.39
$\Delta E_{\text{LUMO-HOMO}}$	4.64	4.89	4.79	3.96	5.17	4.42	5.11	4.49	3.78
Compd.	**H**	**H1**	**H2**	**H3**	**H4**	**H5**	**H6**	**H7**	**H8**
HOMO	-8.00	-8.95	-7.68	-8.71	-7.35	-8.26	-7.05	-8.98	-9.07
LUMO	-3.38	-4.38	-3.48	-4.22	-3.07	-3.67	-2.72	-4.40	-4.50
$\Delta E_{\text{LUMO-HOMO}}$	4.62	4.57	4.20	4.49	4.28	4.59	4.33	4.58	4.57

[a]A-H stand for the unsubstituted compounds.

Figure 1 presents the change tendency of E_{HOMO}, E_{LUMO} and $\Delta E_{\text{LUMO–HOMO}}$ of the designed compounds. For E_{HOMO}: when compounds were substituted by the same energetic group but different bridges, the –CH_2CH_2–(combined with –CN, –NO_2 and –$C(NO_2)_3$ groups), –N=N–(combined with –N_3, –$NHNH_2$ and –$NHNO_2$ groups), –CH=N–(combined with –$CH(NO_2)_2$ group) and –N=CH–(combined with –NH_2 group) bridged compounds have the lowest values of E_{HOMO} while the

–NHNH–(combined with $–NH_2$ group), $–CH_2NH–$(combined with –CN, $–N_3$, $–NO_2$, $–NHNH_2$ and $–NHNO_2$ groups) and $–NHCH_2–$ (combined with $–C(NO_3)_3$ and $–CH(NO_2)_2$ group) substituted ones have the highest values of E_{HOMO}. When compounds were substituted by the same bridge but different energetic groups, the $–C(NO_3)_3$/$–CH(NO_2)_2$ substituted compounds have the lowest values of E_{HOMO} while the $–NH_2$/$–NHNH_2$ substituted compounds have the highest values of E_{HOMO}. The influence order of different energetic groups on E_{HOMO} for series A, B, D, F and H can be written as follows: $–NHNH_2$/$–NH_2$>$–N_3$>$–NHNO_2$>$–NO_2$>–CN/$–CH(NO_2)_2$>$–C(NO_2)_3$ while the influence order was $–NHNH_2$/$–NH_2$>$–N_3$>$–NHNO_2$>$–NO_2$>–CN>$–C(NO_2)_3$ >$–CH(NO_2)_2$ for other series. For E_{LUMO}: when compounds were substituted by the same energetic group but different bridges, series D were found to have the lowest E_{LUMO} which indicates that the addition of –N=N– bridge will decrease the E_{LUMO}. When compounds were substituted by the same bridge but different energetic groups, no evident regularity was found. Overall, the change tendency of E_{HOMO} and E_{LUMO} were approximately the same to each other. In view of $\Delta E_{HOMO-LUMO}$, for compounds with the same energetic group but different bridges, the –N=N– bridged compounds (except for compound G8) have the lowest $\Delta E_{LUMO–HOMO}$ while the $–CH_2CH_2–$ bridged compounds have the highest values of $\Delta E_{HOMO-LUMO}$. It can be predicted that the addition of –N=N– bridge will decrease the stabilities of the designed compounds while the $–CH_2CH_2–$ bridge will act on the opposite side. For compounds with the same bridge but different energetic groups, the $–CH_2CH_2–$, –NHNH–, $–CH_2NH–$ and $–NHCH_2–$ bridges with $–C(NO_2)_3$ substituent possess the lowest values of $\Delta E_{HOMO-LUMO}$ while no regularity was found for the other compounds.

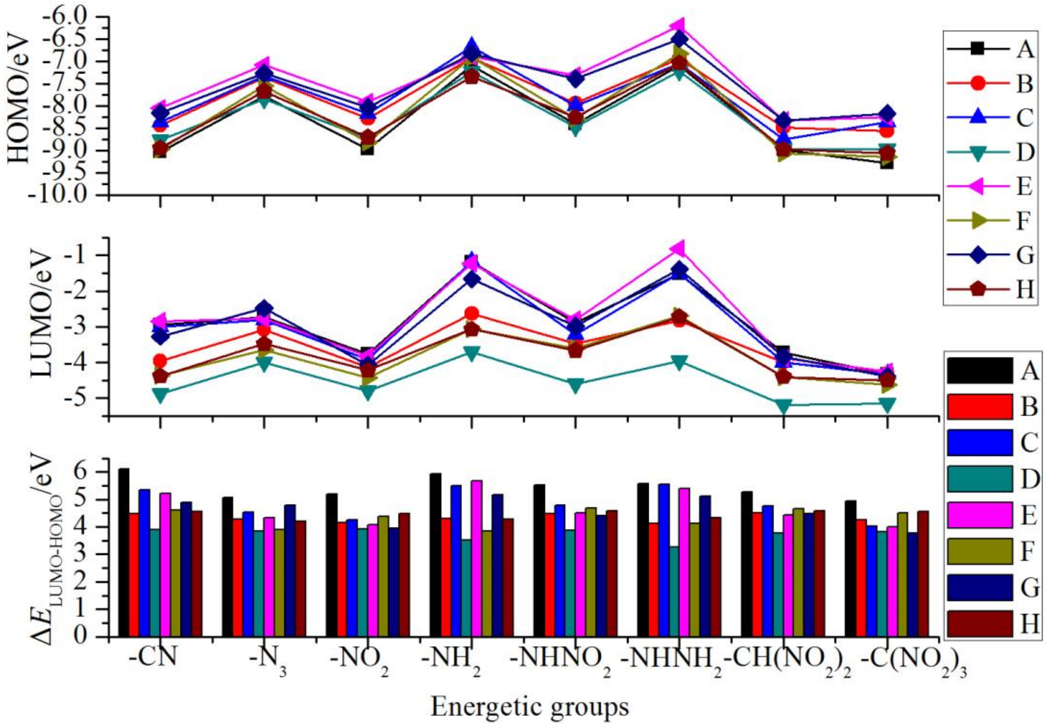

Figure 1. The change tendency of E_{HOMO}, E_{LUMO} and $\Delta E_{LUMO\text{–}HOMO}$ of the designed compounds

2.2 Heats of formation

Heats of formation (ΔH_f), especially the solid-phase heats of formation ($\Delta H_{f,solid}$), is of importance to indicate the energy content of an energetic material. It is also an basic parameter to be considered since compounds with higher positive $\Delta H_{f,solid}$ will lead to higher detonation properties. The calculated total energies (E_0), thermal corrections (H_T), zero point energies (ZPE), molecular properties (A, v and σ^2_{tot}), $\Delta H_{f,gas}$, heats of sublimation (H_{sub}) and $\Delta H_{f,solid}$ of the designed compounds were summarized in Table 2 (the quantitative molecular surface analysis was performed using the Multiwfn program[23]). From the table, it is seen that the all the designed compounds had high positive $\Delta H_{f,solid}$ ranges from 454.7 (A4) to 1506.3 kJ mol^{-1} (D2) which meet the designing concepts of high energy materials. It is also found that the calculated $\Delta H_{f,solid}$ show the same trend as the $\Delta H_{f,gas}$, suggesting that the change trend in the ΔH_f of the designed compounds under the influences of different substituents and bridges drawn from the gas phase results were consistent with those from the solid phase ones. For a comparison, all the designed compounds had higher $\Delta H_{f,solid}$ than those of

1,3,5-trinitro-1,3,5-triazinane (RDX, 79.0 kJmol^{-1}) and 1,3,5,7-tetranitro-1,3,5,7-tetrazocane (HMX, 102.4 kJmol^{-1})^{24} due to the large amount of C-N/N-N energetic bonds and large strain energy of the ring.

Table 2. Calculated total energy (E_0), thermal correction (H_T), zero point energy (ZPE), molecular properties and heat of formation (ΔH_f) of the designed compounds

Compd.	E_0(a.u)	ZPE (kJ mol^{-1})	H_T (kJ mol^{-1})	$\Delta H_{f,gas}$ (kJ mol^{-1})	A (Å^2)	ν	σ^2_{tot} (kcal mol^{-1})^2	ΔH_{sub} (kJ mol^{-1})	$\Delta H_{f,solid}$ (kJ mol^{-1})
A1	-782.371466	331.3	36.9	887.1	236.1	0.183	190.8	115.5	771.6
A2	-925.090161	354.0	42.6	1287.5	258.3	0.248	138.1	127.4	1160.1
A3	-1006.929567	350.7	41.2	615.2	241.0	0.192	169.3	116.7	498.5
A4	-708.603866	430.8	35.2	572.9	219.1	0.232	245.3	118.2	454.7
A5	-1117.649820	440.7	47.2	725.3	270.1	0.169	280.3	141.5	583.8
A6	-819.262128	520.2	41.5	830.4	245.2	0.242	272.4	135.7	694.7
A7	-1494.689032	513.3	61.9	693.8	325.6	0.094	320.8	168.8	525.0
A8	-1903.722760	515.3	76.9	812.3	363.6	0.113	134.5	187.1	625.2
B1	-781.140872	269.1	35.9	999.4	233.0	0.199	155.2	111.5	887.9
B2	-923.862974	292.5	41.1	1391.1	253.6	0.245	127.0	122.8	1268.3
B3	-1005.698088	288.2	40.5	729.9	237.2	0.197	155.6	113.5	616.4
B4	-707.377248	368.4	34.1	674.5	214.4	0.214	289.6	118.2	556.3
B5	-1116.419625	378.6	46.2	836.7	268.9	0.159	277.0	139.1	697.6
B6	-818.033994	456.9	40.9	935.6	244.5	0.226	293.6	135.5	800.1
B7	-1493.453316	449.9	61.6	819.2	329.9	0.074	298.5	166.5	652.7
B8	-1902.489682	453.6	75.6	931.5	361.2	0.122	120.2	184.7	746.8

C1	-814.417167	269.5	36.8	1079.9	227.7	0.129	268.7	111.0	968.9
C2	-957.129364	291.9	42.0	1496.6	250.1	0.229	257.8	135.4	1361.2
C3	-1038.973006	289.3	40.5	813.8	230.4	0.122	272.1	111.5	702.3
C4	-740.653540	370.5	33.6	755.3	203.9	0.208	288.3	112.4	642.9
C5	-1149.700050	381.0	45.8	907.1	252.1	0.178	315.7	135.2	771.9
C6	-851.306251	459.7	40.7	1028.0	231.4	0.233	304.0	130.4	897.6
C7	-1526.728660	451.6	61.2	902.1	316.2	0.098	322.1	163.0	739.1
C8	-1935.771700	454.3	75.9	996.6	359.9	0.099	199.6	187.9	808.7
D1	-813.151548	203.8	35.0	1282.7	222.8	0.185	158.5	105.3	1177.4
D2	-955.891164	227.7	40.0	1628.7	244.7	0.250	155.5	122.4	1506.3
D3	-1037.716668	222.6	39.7	992.2	231.8	0.165	162.5	108.2	884.0
D4	-739.416041	303.1	33.7	884.5	202.5	0.207	297.3	112.4	772.1
D5	-1148.451069	315.0	44.6	1066.5	248.5	0.148	267.3	124.9	941.6
D6	-850.075091	392.8	40.2	1140.4	237.8	0.243	214.3	125.5	1014.9
D7	-1525.488241	385.5	60.7	1039.7	324.8	0.082	221.5	159.8	879.9
D8	-1934.520561	389.0	74.6	1162.3	357.7	0.121	110.7	180.7	981.6
E1	-798.406819	301.3	36.7	952.6	232.7	0.139	231.5	112.1	840.5
E2	-941.124871	324.2	42.3	1354.8	255.5	0.247	157.6	128.5	1226.3
E3	-1022.970765	321.1	40.6	665.4	236.1	0.158	195.4	113.1	552.3
E4	-724.635806	400.9	34.5	647.0	207.5	0.240	1271.3	181.2	465.8
E5	-1133.692227	412.0	46.7	773.3	261.4	0.159	228.7	130.4	642.9
E6	-835.306392	491.1	40.8	872.9	235.8	0.245	274.0	131.1	741.8

E7	-1510.724802	484.1	61.3	758.7	236.1	0.169	208.1	115.7	643.0
E8	-1919.757792	487.3	75.4	879.4	343.5	0.095	181.7	173.0	706.4
F1	-797.167466	236.8	35.5	1089.8	230.1	0.173	216.9	113.9	975.9
F2	-939.890054	259.9	40.9	1480.1	247.4	0.243	147.1	122.1	1358.0
F3	-1021.723120	255.8	40.2	824.4	236.1	0.169	208.1	115.7	708.7
F4	-723.411926	336.1	33.7	743.7	210.5	0.214	281.7	115.6	628.1
F5	-1132.454590	347.2	45.6	905.9	267.0	0.163	257.7	136.9	769.0
F6	-834.066752	425.8	40.1	1010.6	242.6	0.245	304.3	137.8	872.8
F7	-1509.484610	417.8	61.2	897.4	327.7	0.074	313.5	165.7	731.7
F8	-1918.519763	421.2	75.3	1012.7	359.4	0.125	150.3	186.7	826.0
G1	-798.404300	301.6	36.6	959.4	228.9	0.169	232.3	114.3	845.1
G2	-941.124163	325.1	41.5	1356.7	246.4	0.249	208.2	130.0	1226.7
G3	-1022.964040	322.2	40.3	683.8	233.5	0.198	195.0	116.3	567.5
G4	-724.637926	402.1	34.2	642.3	207.0	0.244	354.5	124.5	517.8
G5	-1133.691861	412.6	46.3	774.5	253.0	0.197	252.1	132.6	641.9
G6	-835.304879	492.8	40.0	877.8	230.9	0.249	299.7	131.7	746.1
G7	-1510.717105	483.1	61.5	778.1	303.2	0.102	289.7	152.7	625.4
G8	-1919.750475	486.5	75.5	897.9	337.3	0.134	176.2	173.1	724.8
H1	-797.173226	237.5	35.6	1075.5	229.6	0.177	186.6	111.0	964.5
H2	-939.895745	260.8	40.6	1465.8	249.9	0.249	131.1	121.7	1344.1
H3	-1021.727982	256.2	40.1	811.9	235.4	0.160	176.4	111.0	700.9
H4	-723.408831	335.6	34.4	752.0	210.8	0.216	273.5	115.2	636.8

H5	-1132.459046	348.1	45.5	895.0	266.1	0.156	235.9	133.5	761.5
H6	-834.073986	427.1	39.9	992.7	240.9	0.233	304.5	135.5	857.2
H7	-1509.492062	418.8	61.1	878.7	325.7	0.083	273.4	163.9	714.8
H8	-1918.526392	422.2	75.2	996.2	359.3	0.118	132.9	184.1	812.1

Since energetic materials were always in solid phase rather than gas phase, $\Delta H_{f,solid}$ were selected as the important research object and the effects of different bridges and energetic groups on $\Delta H_{f,solid}$ were displays in Figure 2. From the figure, obvious regulation on the change tendency of $\Delta H_{f,solid}$ was found as follows: (1) for compounds with the same energetic group but different bridges, the –N=N– bridged compounds had the highest $\Delta H_{f,solid}$ while the –CH_2CH_2– bridged compounds have the lowest $\Delta H_{f,solid}$. It is also should be pointed out that compounds with the conjugated bridges have higher $\Delta H_{f,solid}$ values than the corresponding ones with the unconjugated bridges. The results may be caused by the large conjugated system that comprised by 1,2,5-oxadiazole, 1,2,3,4-tetrazole and the conjugated bridges together. (2) for compounds with the same bridge but different energetic groups, it is found that the –N_3 substituted compounds had the highest $\Delta H_{f,solid}$ while the –NH_2 substituted compounds had the lowest $\Delta H_{f,solid}$. In other words, –N_3 was the most effective group in improving $\Delta H_{f,solid}$ of the 1,2,5-oxadiazole-1,2,3,4-tetrazole based compounds while the –NH_2 group will make less contribution to these values. The influence sequence of different energetic groups on $\Delta H_{f,solid}$ can be written as follows: –N_3>–CN>–$NHNH_2$>–$C(NO_2)_3$>–$NHNO_2$>–$CH(NO_2)_2$>–NO_2>–NH_2 (for series A, B, C, F, G and H). Overall, it is concluded that −N_3 group and –N=N– bridge acted as the most effective group/bridge in improving $\Delta H_{f,solid}$ of the designed compounds than the other groups/bridges, suggesting that the −N_3 and –N=N− group/ bridge should be given great attention when a high energy material was designed.

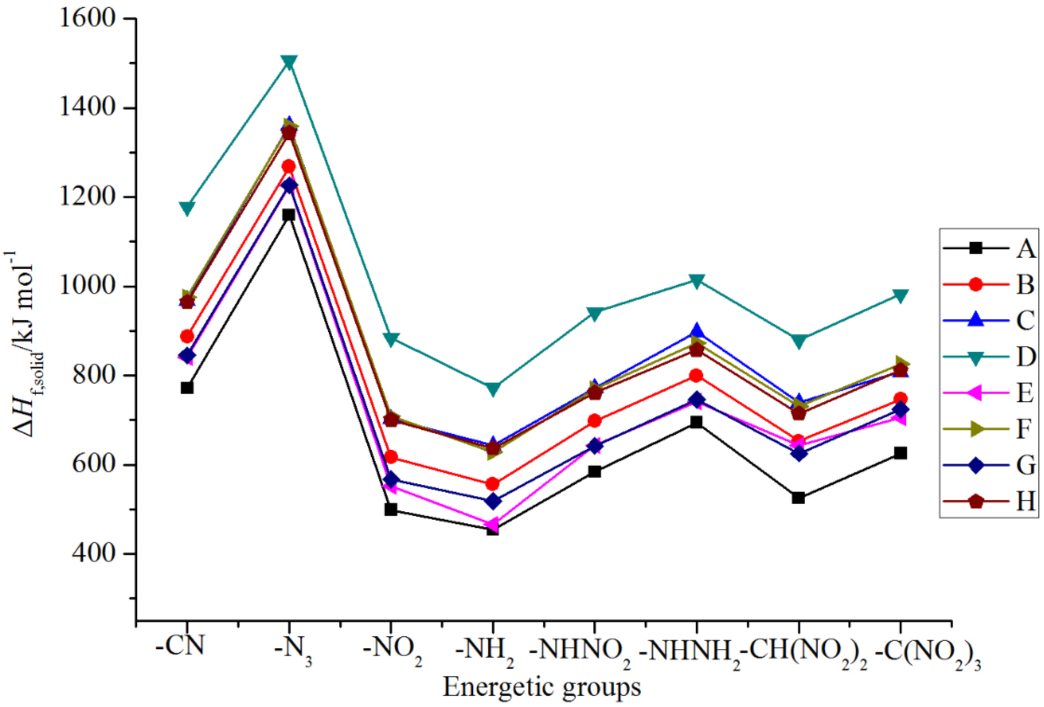

Figure 2. The change tendency of HOFs of the designed compounds

2.3 Detonation properties

Oxygen balance (OB), density (*ρ*), heats of detonation (*Q*), detonation velocities (*D*) and detonation pressure (*P*) were calculated and summarized in Table 3. Usually, these parameters always acted as important indicators to measure the "energy contents" of an energetic material.[25] In addition, the related values of RDX and HMX were also listed in the table to give a full comparison. From the table, it is observed that values of OB, *ρ*, *Q*, *D* and *P* were from -111.11 (A1) to 10.34 (D8), from 1.48 (A4 and A6) to 1.99 g cm^{-3} (D8), from 783.3 (B4) to 1863.71 cal g^{-1}(H5), from 6.26 (B1) to 9.52 km s^{-1} (G8) and from 15.7 (A1) to 42.1 GPa (G8), respectively. Previous research have demonstrated that too much or less oxygen is not favorable for improving explosive performance of high energy materials. This is because these high energy materials can not be combusted fully under oxygen-deficient situation and the additional oxygen will produce O_2 which may take away a great deal of energy under oxygen-surficient situation. Not surprisingly, OB of compounds E8, F8, G8 and H8 were close to zero, suggesting that the combination of $–CH_2NH–$, –CH=N–, /$–C(NO_2)_3$ may be the best choice in balancing values of OB. For values of *ρ*, 17 compound (A8, B8, C3, C7, C8, D3, D5, D7, D8, E7, E8, F7, F8, G7, G8, H7 and H8) possess higher values of *ρ* than RDX while only 7 compounds (B8, C8, D8, E8, F8, G8 and H8) have higher values of *ρ* than HMX. For values of *Q*, 20 compounds (A8,

B7, B8, C3, C7, D2, D3, D5, D7, E7, E8, F3, F7, F8, G7, G8, H3, H5, H7 and H8) possess higher *Q* than RDX while 22 compounds have higher *Q* than HMX (A8, B8, C7, D2, D5, D7, E8, F7, F8, G8, H5, H7 and H8). In view of *D*, there were 18 compounds (A8, B8, C3, C5, C7, C8, D3, D5, D7, D8, E8, F7, F8, G7, G8, H5, H7 and H8) have higher/equal values compared to that of RDX while 10 compounds (A8, B8, C8, D3, D7, D8, E8, F8, G8 and H8) possess higher values than HMX. In addition, there were 19 compounds (A8, B8, C3, C5, C7, C8, D3, D5, D7, D8, E7, E8, F7, F8, G7, G8, H5, H7 and H8) had higher values than RDX while 7 compounds (B8, C8, D8, E8, F8, G8 and H8) possess higher values than HMX.

Table 3. Calculated oxygen balance (OB), densities (*ρ*), heats of detonation (*Q*), detonation velocities (*D*) and detonation pressures (*P*) of the designed compounds

Compound	OB[a]	ρ (g cm^{-3})	Q (cal g^{-1})	D (km s^{-1})	P (GPa)
A1	-111.11	1.52	1121.35	6.28	15.7
A2	-70.97	1.60	1351.06	7.46	22.9
A3	-43.75	1.73	1468.03	8.04	28.0
A4	-106.12	1.48	849.35	6.54	16.7
A5	-44.76	1.70	1423.00	8.01	27.5
A6	-99.12	1.48	990.41	7.03	19.4
A7	-34.22	1.78	1553.54	8.41	31.2
A8	-10.34	1.90	1685.99	9.18	38.6
B1	-104.67	1.55	1261.72	6.26	15.8
B2	-65.04	1.64	1467.17	7.50	23.5
B3	-37.80	1.77	1548.11	8.20	29.5
B4	-98.97	1.52	783.3	6.69	17.8
B5	-39.44	1.73	1490.85	8.15	28.8
B6	-92.86	1.51	1111.71	7.16	20.3
B7	-30.11	1.79	1614.97	8.47	31.7
B8	-6.93	1.92	1732.87	9.27	39.6
C1	-73.39	1.62	1327.37	7.12	21.0
C2	-38.40	1.70	1532.51	8.25	29.2
C3	-12.40	1.85	1603.68	9.02	36.7
C4	-64.65	1.61	1067.95	7.62	24.0
C5	-16.67	1.81	1531.80	8.89	35.1

C6	-63.16	1.59	1194.41	7.98	26.2
C7	-12.77	1.86	1652.71	9.09	37.4
C8	6.87	1.97	1547.92	9.39	41.2
D1	-66.67	1.66	1520.48	7.40	23.1
D2	-32.26	1.74	1641.25	8.47	31.2
D3	-6.25	1.87	1743.75	9.21	38.5
D4	-57.14	1.64	1236.39	7.75	25.2
D5	-11.19	1.83	1646.65	9.06	36.8
D6	-56.64	1.61	1329.03	8.07	26.9
D7	-8.56	1.87	1722.72	9.17	38.2
D8	10.34	1.99	1519.08	9.34	41.0
E1	-92.17	1.57	1192.07	6.65	18.0
E2	-54.62	1.65	1409.18	7.81	25.6
E3	-28.02	1.79	1491.39	8.46	31.7
E4	-85.28	1.55	858.51	6.90	19.2
E5	-30.66	1.75	1448.49	8.39	30.7
E6	-81.06	1.54	1035.64	7.43	22.2
E7	-23.47	1.82	1610.24	8.76	34.3
E8	-1.72	1.95	1712.51	9.51	42.0
F1	-85.58	1.60	1328.62	6.74	18.7
F2	-48.58	1.69	1526.21	7.94	26.9
F3	-21.96	1.82	1607.42	8.65	33.4
F4	-77.95	1.58	1066.24	7.15	20.9
F5	-25.26	1.77	1526.59	8.51	31.8
F6	-74.67	1.56	1184.00	7.56	23.1
F7	-19.30	1.83	1646.82	8.79	34.6
F8	1.73	1.96	1707.59	9.48	41.8
G1	-92.17	1.57	1197.14	6.66	18.1
G2	-54.62	1.65	1409.56	7.81	25.7
G3	-28.02	1.79	1505.53	8.48	31.8
G4	-85.28	1.55	921.60	7.02	19.9
G5	-30.66	1.76	1447.65	8.49	31.7
G6	-81.06	1.55	1040.17	7.47	22.5

G7	-23.47	1.82	1599.02	8.75	34.1
G8	-1.72	1.95	1721.97	9.52	42.1
H1	-85.58	1.60	1315.94	6.77	18.6
H2	-48.58	1.69	1512.76	7.93	26.8
H3	-21.96	1.82	1600.11	8.64	33.3
H4	-77.95	1.57	1076.90	7.14	20.7
H5	-25.26	1.78	1863.71	8.98	35.5
H6	-74.67	1.56	1167.43	7.53	23.0
H7	-19.30	1.83	1635.99	8.78	34.5
H8	1.73	1.96	1700.41	9.45	41.8
RDX[26]	-21.6	1.82	1590.7	8.75	34.0
HMX[26]	-21.6	1.91	1633.9	9.10	39.0

[a] For the explosive $C_aH_bO_cN_d$: OB = (c-2a-0.5b)/M_w, where M_w is the molecular weight.

Figure 3 (a)-(d) illustrates the change tendency of ρ, Q, D and P of the designed compounds, respectively. It is seen that the change tendency of ρ, D and P of the designed compounds were approximately the same to each other while those of Q was different. For compounds substituted by the same energetic group but different bridges, the influence of different bridges on values of ρ can be written in the following order: –N=N–>–NHNH–>–N=CH–≥–CH=N>–$NHCH_2$–≥–CH_2NH–>–CH=CH–>–CH_2–CH_2–. However, for compounds substituted by the same bridge but different energetic groups, evident influence sequence for series A-H were found as follows: –$C(NO_2)_3$>–$CH(NO_2)_2$≥–NO_2>–$NHNO_2$>–N_3≥–CN>–NH_2≥–$NHNH_2$. It can be concluded that the –N=N–/–$C(NO_2)_3$ substituents were acted as the most effective substituents in improving values of ρ while –CH_2–CH_2–/–$NHNH_2$/–NH_2 will make less contribution to ρ. In view of Figure 3(b)-(d), when the designed compounds were substituted by the same energetic group but different bridges, the –N=N– bridged compounds possess the highest values of Q, D and P (except for the –($C(NO_2)_3$ substituted compounds) while the –CH_2–CH_2– bridged ones have the lowest value (except for the –CN, –NH_2 and –$C(NO_2)_3$ substituted compounds). It indicates that the –N=N– bridge was more effective in improving the Q, D and P of the designed compounds rather than other bridges. The detailed influence sequences of different bridges on Q, D and P were as follows: (1) for values of Q:

–N=N–>–CH=N–/–NHNH–>–N=CH–>–CH=CH–>–CH_2NH–>–NHCH_2–>–CH_2CH_2– (except for the –CN, –CH$(NO_2)_2$ and –NHNO_2 substituted compounds); (2) for values of *D*: –N=N–>–NH–NH–>–N=CH–/–CH=N–>–NHCH_2–/–CH_2NH–>–CH=CH–>–CH_2–CH_2– (except for the –CN and –C$(NO_2)_3$ substituted compounds); (3) for values of *P*: –N=N–>–NH–NH–>–N=CH–/–CH=N–>–NHCH_2–/–CH_2NH–>–CH=CH–>–CH_2–CH_2– (only for the –C$(NO_2)_3$ substituted compounds). No regularity was found for the other substituted compounds. It is also interesting to found that compounds with the conjugated bridges have higher *D* or *P* than the corresponding ones with the unconjugated bridges. When compounds were substituted by the same bridge but different energetic groups, the influence sequence of different energetic groups on *Q* were in the following order: –C$(NO_2)_3$>–CH$(NO_2)_2$>–NO_2>–NHNO_2>–N_3>–CN>–NHNH_2>–NH_2 (except for series C and D). The influence sequence of different energetic groups on *P* were written as follows: : –C$(NO_2)_3$>–CH$(NO_2)_2$>–NO_2>–NHNO_2>–N_3>–NHNH_2>–NH_2>–CN. Additionally, the influence sequences of different energetic groups on *P* were observed to be the same to that of *D* (except for series D), indicating that compounds with higher *D* will always possess higher *P*. Overall, –N=N–/–C$(NO_2)_3$ substituents were selected as the most effective substituents in improving the values of *D* and *P* while –CH_2–CH_2–/-CN substituents acted on the opposite side.

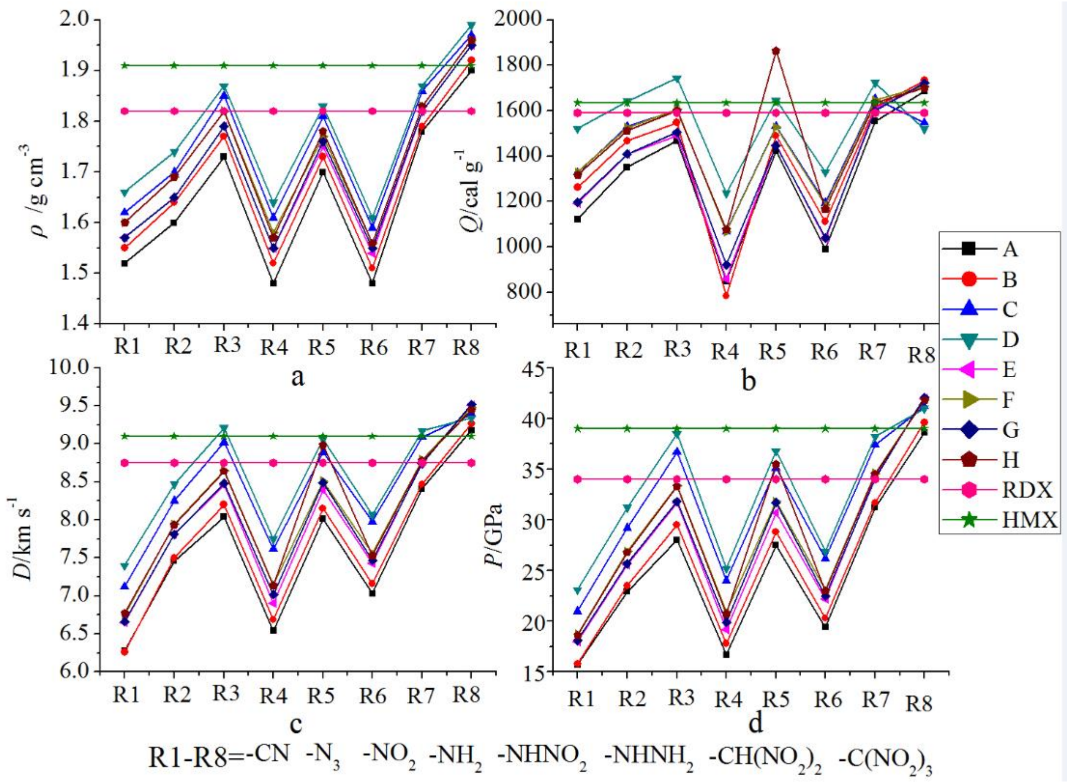

Figure 3. The change tendency of *ρ*, *Q*, *D* and *P* of the designed compounds

2.4 Thermal stabilities

Bond dissociation energy (BDE) was another important factor to be investigated since it can provide lots of useful information on thermal stability, pyrolysis mechanism, and enhancing controllability of kinetic energy release of high energy materials.[27] It has also demonstrated that the smaller is the energy for breaking an energetic bond, the weaker the bond is, and the easier the bond becomes a trigger bond. In order to screen the trigger bonds and elucidate the pyrolysis mechanism of the designed compounds, natural bond orbital (NBO) analyses were carried out to obtain the Wiberg bond index (WBI, a smaller WBI of a chemical bond always indicates as a potential trigger bond). Then, seven possible trigger bonds and the corresponding bond dissociation energies were calculated: (1) ring (C) –R; (2) ring (N) –R; (3) C–C (bridge); (4) C–N (bridge); (5) C–O (bridge); (6) N–N or N=N (bridge); (7) NH–NH_2 or NH–NO_2 or C–NO_2. The predicted BOs and their corresponding BDEs were summarized in Table 4. From the table, it is seen that compounds with higher/lower BO values didn’t possess higher /lower values of BDEs, indicating that there was no inevitable relation between values of BO and BDE for different compounds. It is also found that ring (N)–R was selected as the trigger bond for compounds A2, A3, A6, B1-B4, B6, C3, C6, D2, D4, D6, E2, E3, F2, F3, F4, F6, G2, G3, G6, H2, H3, H4 and

H6 while ring (C)-R selected as the trigger bonds for none of the designed compounds. However, the bridges were selected as the trigger bonds for compounds A1, A4, C1, C2, C4, D1, D3, E1, E4, F1, G1, G4 and H1 while NH–NH_2/NH–NO_2/C–NO_2 chemical bonds will be more unstable for compounds A5, A7, A8, B5, B7, B8, C5, C7, C8, D5, D7, D8, E5, E6, E7, E8, F5, F7, F8, G5, G7, G8, H5, H7 and H8.

Table 4. Bond dissociation energies (BDE, kJ mol^{-1}) for the weakest bonds of the designed compounds.

Compd.	Ring(C)-R		Ring(N)-R		C-C/C=C(bridge)		C-N/C=N(bridge)		N-N/N=N(bridge)		NH-NH_2/NH-NO_2/C-NO_2	
	BO	BDE	BO	BDE	BO	BDE	BO	BDE	BO	BDE	BO	BDE
A1	1.0782	552.4	1.0512	448.2	1.0067	247.0	--	--	--	--	--	--
A2	1.0764	362.0	1.0152	194.3	0.9969	248.7	--	--	--	--	--	--
A3	0.9189	255.9	0.8721	132.7	0.9937	247.3	--	--	--	--	--	--
A4	1.1250	449.8	1.0329	304.1	0.9875	250.5	--	--	--	--	--	--
A5	1.0328	418.7	1.0549	262.0	0.9949	253.6	--	--	--	--	0.9147	100.3
A6	1.1268	360.5	1.0130	204.4	0.9795	252.2	--	--	--	--	1.0341	207.6
A7	0.9900	365.5	1.0066	453.4	0.9969	261.8	--	--	--	--	0.8135	138.0
A8	1.0140	454.9	1.0124	366.3	1.0032	253.7	--	--	--	--	0.7796	110.5
B1	1.0784	548.5	1.0520	407.4	1.0946	500.1	--	--	--	--	--	--
B2	1.0082	362.7	1.0203	152.7	1.0971	506.4	--	--	--	--	--	--
B3	0.9144	249.3	0.8568	92.9	1.0900	325.6	--	--	--	--	--	--
B4	1.1408	451.5	1.0337	258.9	1.1010	501.2	--	--	--	--	--	--
B5	1.0382	416.3	1.0563	222.1	1.0902	497.7	--	--	--	--	0.8944	101.0
B6	1.1408	361.4	1.0123	155.8	1.1016	503.5	--	--	--	--	1.0349	230.9
B7	1.0099	435.2	0.9915	321.2	1.0909	497.1	--	--	--	--	0.8121	136.2
B8	1.0140	448.2	1.0107	323.7	1.0862	491.1	--	--	--	--	0.8001	111.8
C1	1.0841	553.4	1.0661	387.6	--	--	1.0993	348.2	1.0313	186.6	--	--
C2	1.0829	356.1	1.0093	131.9	--	--	1.0848	351.2	1.0248	150.8	--	--
C3	0.9358	267.7	0.8591	56.9	--	--	1.1158	346.2	1.0171	174.4	--	--
C4	1.1675	465.5	1.0385	249.3	--	--	1.0360	364.2	1.0141	151.0	--	--
C5	1.0373	427.5	1.0586	202.7	--	--	1.0958	372.5	1.0123	167.6	0.9021	110.3
C6	1.1284	354.5	0.9999	132.4	--	--	1.0200	366.1	1.0038	136.3	1.0355	219.4
C7	1.0044	448.7	0.9902	307.3	--	--	1.0106	366.6	1.0077	165.3	0.8069	136.4
C8	1.0223	463.7	1.0282	309.0	--	--	1.1164	362.7	1.0179	203.1	0.7654	106.9
D1	1.0766	546.5	1.0405	309.9	--	--	1.0651	243.4	1.8779	504.8	--	--
D2	1.1063	352.3	1.0256	137.9	--	--	1.1246	292.2	1.7306	433.5	--	--
D3	0.9080	240.2	0.7904	301.1	--	--	1.0825	273.5	1.7864	383.2	--	--
D4	1.2154	471.4	1.0320	256.9	--	--	1.1123	300.3	1.6957	507.0	--	--
D5	1.0507	416.5	1.0517	229.6	--	--	1.0823	158.2	1.7567	626.2	0.8551	96.3
D6	1.1844	378.7	1.0047	157.8	--	--	1.1282	305.6	1.7154	285.1	1.0366	204.9
D7	1.0075	443.0	0.9777	367.7	--	--	1.1083	289.2	1.7515	533.6	0.8182	137.0

D8	1.0101	451.0	0.9939	365.1	--	--	1.0962	279.0	1.7711	460.8	0.7793	131.1
E1	1.0853	555.6	1.0502	447.1	1.0024	403.2	0.9876	248.8	--	--	--	--
E2	1.0754	356.3	1.0174	191.1	1.0112	404.0	0.9624	240.6	--	--	--	--
E3	0.9367	268.6	0.8708	36.8	1.0032	397.4	0.9831	262.5	--	--	--	--
E4	1.1133	434.0	1.0274	296.3	1.0083	401.7	0.9741	231.9	--	--	--	--
E5	1.0313	424.7	1.0534	278.4	1.0001	403.8	0.9647	252.3	--	--	0.8700	96.6
E6	1.0907	359.5	1.0084	217.8	0.9989	407.6	0.9664	245.6	--	--	1.0281	196.4
E7	1.0140	439.6	0.9832	366.6	1.0026	409.5	0.9604	265.9	--	--	0.8193	146.2
E8	1.0249	458.6	1.0007	354.8	1.0015	382.5	0.9613	253.7	--	--	0.7772	101.3
F1	1.0772	548.8	1.0479	416.1	1.0712	452.5	1.1099	385.9	--	--	--	--
F2	1.1083	359.0	1.0223	166.0	1.0879	466.6	1.1150	392.1	--	--	--	--
F3	0.9093	244.3	0.8389	41.1	1.0614	446.0	1.1100	380.6	--	--	--	--
F4	1.1713	465.6	1.0322	268.7	1.0796	468.2	1.1150	397.2	--	--	--	--
F5	1.0426	418.0	1.0538	253.3	1.0674	459.4	1.1055	383.1	--	--	0.8519	93.5
F6	1.1117	347.8	1.0102	185.1	1.0733	462.0	1.1075	376.0	--	--	1.0278	209.8
F7	1.0092	448.5	0.9858	329.2	1.0763	447.0	1.1063	395.8	--	--	0.8140	135.2
F8	1.0119	458.1	1.0060	266.7	1.0634	437.2	1.1053	387.0	--	--	0.7761	112.3
G1	1.0784	550.8	1.0663	378.6	0.9988	385.8	0.9654	228.8	--	--	--	--
G2	1.0822	365.3	1.0074	119.1	0.9995	396.2	0.9685	227.0	--	--	--	--
G3	0.9193	262.0	0.8880	57.3	0.9970	402.5	0.9648	240.5	--	--	--	--
G4	1.1240	449.4	1.0330	229.2	0.9996	389.0	0.9672	224.6	--	--	--	--
G5	1.0368	426.3	1.0657	209.1	0.9998	392.7	0.9763	243.5	--	--	0.8594	94.0
G6	1.1070	362.6	1.0155	143.3	1.0004	399.3	0.9776	241.7	--	--	1.0295	213.5
G7	1.0070	437.0	1.0000	291.5	1.0069	388.8	0.9673	213.9	--	--	0.8031	140.9
G8	1.0162	454.3	1.0309	284.9	1.0018	376.4	0.9681	213.3	--	--	0.7833	98.1
H1	1.0775	545.0	1.0429	411.8	1.0758	453.0	1.1308	404.3	--	--	--	--
H2	1.0929	363.0	1.0243	159.3	1.0821	460.0	1.1344	407.9	--	--	--	--
H3	0.9116	246.8	0.8360	90.2	1.0593	453.0	1.1280	389.4	--	--	--	--
H4	1.1482	453.1	1.0357	266.3	1.0918	454.1	1.1235	404.4	--	--	--	--
H5	1.0427	415.7	1.0553	243.9	1.0684	451.3	1.1257	405.2	--	--	0.9567	111.4
H6	1.1189	359.8	1.0124	182.3	1.0816	457.4	1.1248	403.3	--	--	1.0301	217.7
H7	1.0097	431.3	0.9848	343.2	1.0734	451.4	1.1216	414.0	--	--	0.8168	139.8
H8	1.0132	444.1	1.0000	339.5	1.0644	445.7	1.1220	399.4	--	--	0.7798	116.8

Figure 4 illustrates the change tendency of BOs and BDEs of the designed compounds. From the figure, it is seen that the change tendency of BOs were similar to each to other. It is also found that BOs of the –CN substituted compounds were more dispersed while those of –NHNH$_2$ and –CH(NO$_2$)$_2$ substituted compounds were more centralized. The results show that bridges were the main influence factor for the –CN substituted compounds, whereas the energetic groups acted as the key elements for the –NHNH$_2$ and –CH(NO$_2$)$_2$ substituted compounds. In view of BDEs, for compounds with the same energetic group but different bridges, it is found that the –NH–NH– bridged compounds have the lowest values of BDEs (for –CN, $–NHNH_2$ and $–NH_2$ substituted compounds) while it is the $–CH_2NH–$/–CH=N–/–N=CH– bridged compounds possess the lowest BDEs for the other substituted compounds. However, no efficient influence sequence was found for the designed compounds. When compounds were substituted by the same bridge but different energetic groups, the –CN substituted compounds were found to have the highest values of BDEs (except for series A, D and E, the fact is that the $–NH_2$ substituted ones has the highest values of BDEs). On the opposite side, the $–NO_2$ substituted compounds has the lowest values of BDEs for series B, C, E, F, G and H while the $–NHNO_2$ substituted has the lowest values of BDEs for series A and D. This is because these molecules contain strong electron withdrawing group which will damage their stabilities to a certain extent. It is also should be noted that the trigger bonds were $NH–NO_2$/$C–(NO_2)_3$/$CH–(NO_2)_2$ rather than other chemical bonds when $–NHNO_2$/$–C(NO_2)_3$/$–CH(NO_2)_2$ groups were added to the parent molecules. Overall, it may be predicted that the –CN/$–NH_2$ will be helpful to improve the thermal stabilities of the designed compounds while the –NH–NH–/$–NO_2$/$–NHNO_2$ substituents will decrease their thermal stabilities for most of the designed compounds.

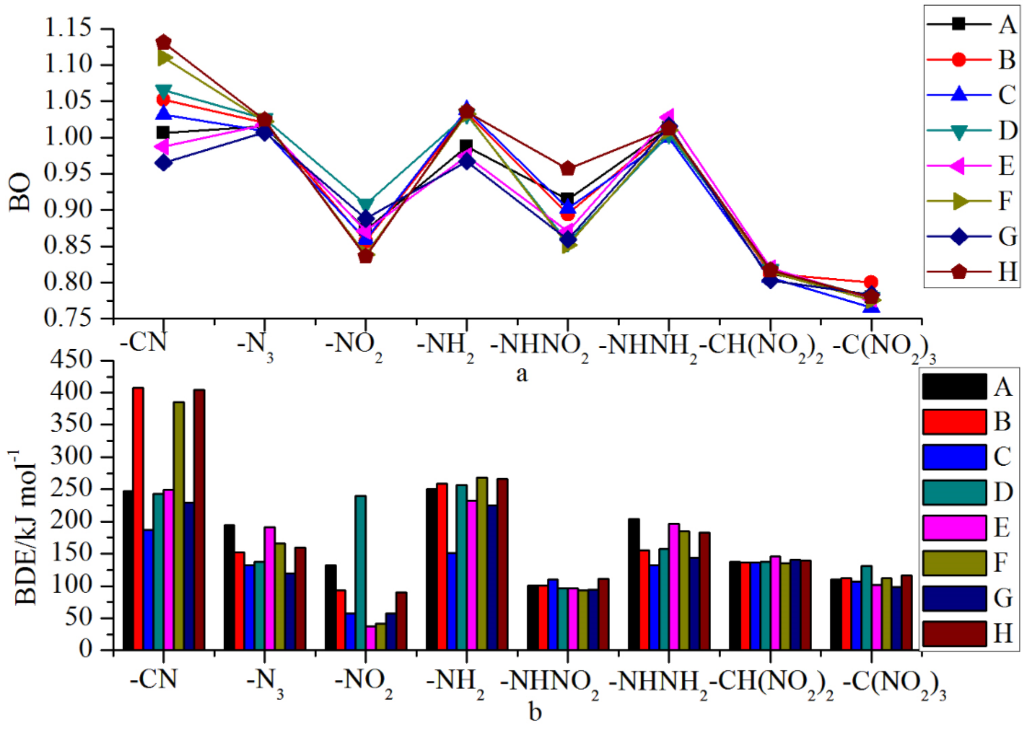

Figure 4. The change tendency of BOs and BDEs of the designed compounds

In general, promising high energy materials should not only have excellent detonation velocities and detonation pressures, but should possess acceptable thermal stabilities. Take both detonation properties and thermal stabilities into consideration, compounds C7, D3, D7, F7, G7 and H7 were finally screened as potential high energy materials since these compounds had superior detonation properties and thermal stabilities than those of RDX (*D*, 8.75 km s^{-1}; *P*, 34.0 GPa; BDE, 134.7 kJ mol^{-1}). Then, electronic structures (such as the distribution of HOMOs and LUMOs, electrostatic potentials) were simulated fully to give a better understanding of physicochemical properties of the screened high energy materials.

2.5 Electronic structures

Figure 5 displays the distribution of the HOMOs and LUMOs, in which the red color represents positive phase and green color represents the negative phase. From the figure, it is clear that the distribution of HOMOs and LUMOs were different from each other. For compound C7, LUMOs were mainly distributed on the $–CH(NO_2)_2$ group that attached to tetrazole ring while the HOMOs were distributed on the tetrazole ring. For compound H3, the distributions were similar to each other and all the orbitals were decentralized on the whole molecule. For compounds D7, F7 and H7, all the orbitals were mainly distributed on the parent molecule. In view of compound G7, the LUMO was mainly distributed on the $–CH(NO_2)_2$ group while the HOMO was mainly distributed on the tetrazole ring. On the other hand, the calculated $\Delta E_{\text{LUMO-HOMO}}$ of compounds C7, D3, D7, F7, G7 and H7 were 4.77, 3.92, 3.78, 4.66, 4.49 and 4.58 eV. It can be predicted that the order of stability were C7>F7> H7>G7>D3>D7 which was also the reverse order of chemical reactivity.

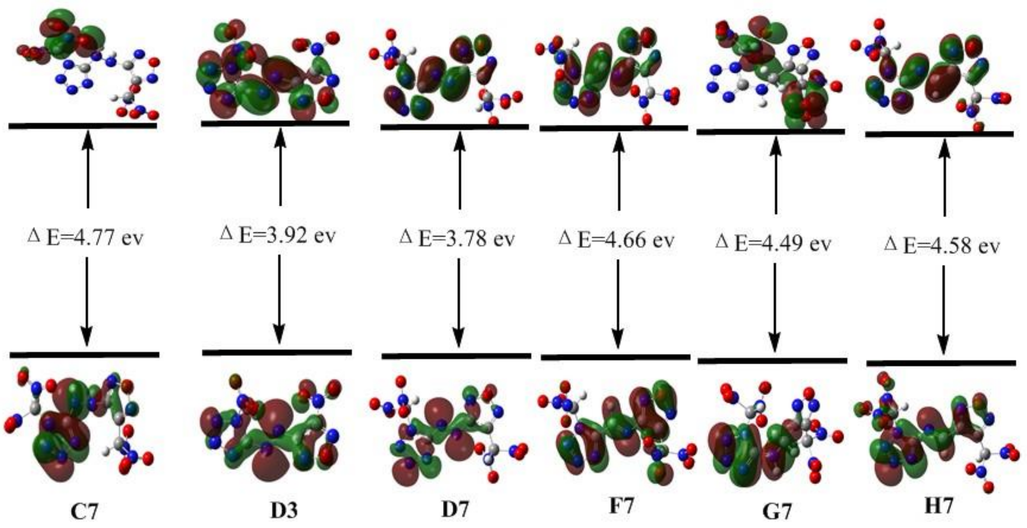

Figure 5 Distribution of LUMO and HOMO of the selected compounds

Electrostatic potential (ESP) on molecular surface[28] of the designed compounds were fully investigated and depicted in Figure 6. It also should be pointed out that the red color presents the positive potentials while the green color presents the negative potentials. It is seen that the positive potentials of the selected compounds were mainly located on the on the oxadiazole/tetrazole ring or bridges while those of negative potentials were mainly distributed on the energetic groups. In order to predict the chemical reactive sites of the designed compounds, the extreme value points of ESP on molecular surface were plotted (only significant surface local minima (blue points) and maxima (red points) were labeled). It is observed that the maximum points for the selected compounds were located around the hydrogen atoms for compounds C7, D7, F7, G7 and H7 with values of +65.7, +55.6, +71.2, +59.9, and +65.9 kcal mol^{-1}. However, the minimum points of compounds C7, D7, F7, G7 and H7 were around nitrogen atoms of tetrazole ring with values of -23.4, -22.6, -23.3, -27.8 and -25.7 kcal mol^{-1}. But for compound D3, the case is that the maximum and minimum points were located near the nitrogen atoms of tetrazole ring with values of +42.6 and -24.8 kcal mol^{-1}, respectively. In view of the area ratios of positive potentials and negative potentials, areas of positive potentials for all the screened compounds were found to be larger than the negative areas which in turn will improve the stabilities of these structures.

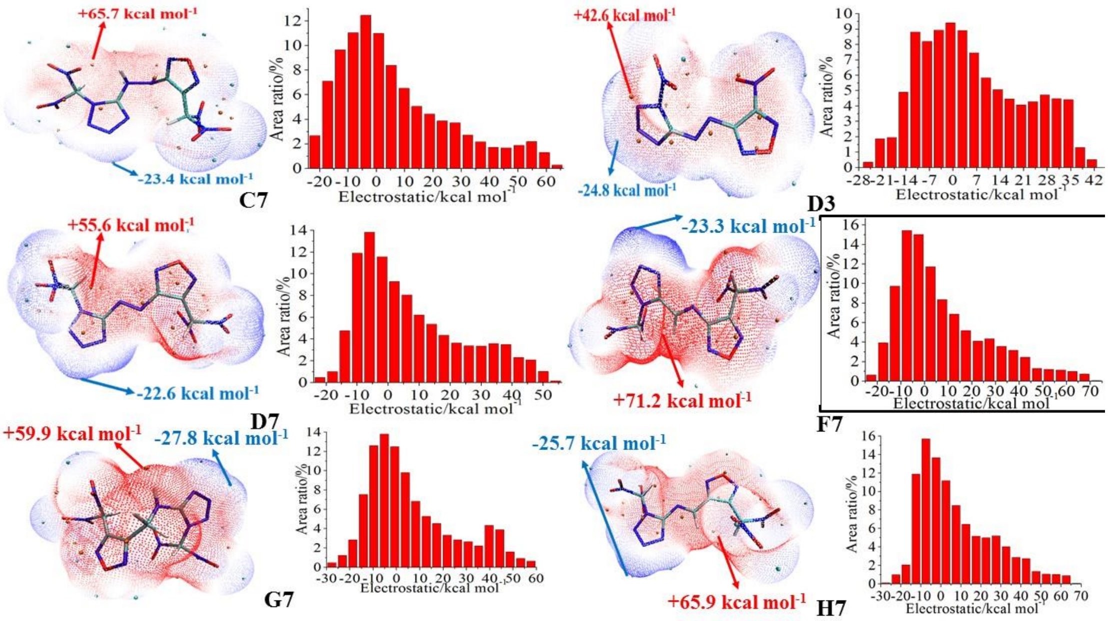

Figure 6 ESP and ratios of the positive and negative potentials of the selected compounds

Conclusions

In this work, 1,2,5-Oxadiazole-1,2,3,4-tetrazole bridged high energy density materials with different energetic groups were designed and their properties were investigated by density functional theory. The values of solid phase of heats of formation were from 454.7 (A4) to 1506.3 kJ mol^{-1} (D2) and the –N=N–/–N_3 substituents were found to be more helpful to improve the heats of formation of the designed compounds. The predicted density, heats of detonation, detonation velocities and detonation pressures were from 1.48 (A4 and A6) to 1.99 g cm^{-3} (D8), from 783.3 (B4) to 1863.71 cal g^{-1}(H5), from 6.26 (B1) to 9.52 km s^{-1} (G8) and from 15.7 (A1) to 42.1 GPa (G8), respectively, indicating that compounds with higher heats of detonation will always possess detonation properties. Based on the calculated bond orders and bond dissociation energies of the weakest bonds, no evident regularity was found for the influence of different substituents/bridges on bond orders while it is true that the NH–NO_2/C–$(NO_2)_3$/CH–$(NO_2)_2$ bonds acted as the trigger bonds. Take both thermal stabilities and energetic properties into consideration, six compounds (C7, D3, D7, F7, G7 and H7) were selected as potential candidates for high energy compounds and their distribution of frontier molecular orbitals and electrostatic potentials were simulated to supply detailed information on their electronic structures.

Acknowledgements

This study was supported by the National Natural Science Foundation of China (Grant No. 11602121) and the Program for Scientific Research Innovation Team in Colleges and Universities of Jinan (No.2018GXRC006).

Supporting Information

The detailed computational methods can be found in the supporting information.

References

1. Hermann, T. S.; Karaghiosoff, K.; Klapötke, T. M.; Stierstorfer, J. Synthesis and Characterization of 2,2′-Dinitramino-5,5′-Bi(1-oxa-3,4-diazole) and Derivatives as Economic and Highly Dense Energetic Materials. *Chem. Eur. J.* **2017**, *23*, 12087-12091.
2. Zhang, C.; Sun, C. G.; Hu, B. C.; Lu, M. Synthesis and Characterization of the Pentazolate Anion Cyclo-N_5 in $(N_5)_6(H_3O)_3(NH_4)_4Cl$. *Science* **2017**, *355*, 374-376.
3. Zhang, Y. Y.; Li ,Y. N.; Yu, T.; Liu, Y. Z.; Chen, S. P.; Ge, Z. X.; Sun,C. H.; Pang,

S. P. Synthesis and Properties of Energetic Hydrazinium 2 5-Nitro-3-dinitromethyl-2H-pyrazole by Unexpected Isomerization of N 3 -Nitropyrazole[J]. *Acs Omega*, **2019**, *21*, 19011-19017.

4. Peng, Y. J.; Jiang, Y. X.; Peng, X.; Liu, J. Y.; Lai, W. P.; Reaction Mechanism of 3, 4-Dinitrofuroxan Formation from Glyoxime: Dehydrogenation and Cyclization of Oxime. *ChemPhysChem* **2016**, *17*, 541-547.
5. Tsyshevsky, R.; Smirnov, A. S.; Kuklja, M. M. Comprehensive End-To-End Design of Novel High Energy Density Materials: III. Fused Heterocyclic Energetic Compounds. *J. Phys. Chem. C* **2019**, *123*, 8688-8698.
6. Qu, Y.; Babailov, S. P. Azo-Linked High-Nitrogen Energetic Materials. *J. Mater. Chem. A* **2018**, *6*, 1915-1940.
7. Dalinger, I. L.; Kormanov, A. V.; Suponitsky, K. Y.; Muravyev, N. V.; Sheremetev, A. B. Pyrazole-Tetrazole Hybrid with Trinitromethyl, Fluorodinitromethyl, or (Difluoroamino) Dinitromethyl Groups: High-Performance Energetic Materials. *Chem. Asian J.* **2018**, *13*, 1165-1172.
8. Jin, X. H.; Xiao, M. H.; Wang, C. Y.; Zhang, C.; Zhou, J. H.; Hu, B. C. Synthesis and Properties of Energetic Materials Based on 1,3-Diazocyclopentane. *Eur. J. Org. Chem.* **2019**, *2019*, 988-994.
9. Dharavath, S.; Shreeve, J. M. A Safer Synthesis of 3,5-Bis(dinitromethyl)-1,2,4-triazole (BDT) and Its Mono and Di Salts: High-Performance Insensitive Energetic Materials. *Propellants, Explos. Pyrotech.* **2018**, *43*, 48-53.
10. Tang, Y. X.; He, C. L.; Imler, G. H.; Parrish, D. A.; Shreeve, J. M. Energetic Furazan-Triazole Hybrid with Dinitromethyl and Nitramino Groups: Decreasing Sensitivity via the Formation of A Planar Anion. *Dalton Trans.* **2019**, *48*, 7677-7684.
11. Lin, H.; Yang, D. D.; Lou, N.; Zhu, S. G.; Li, H. Z.; Computational Design of High Energy Density Materials with Zero Oxygen Balance: A Combination of Furazan and Piperazine Rings. *Comput. Theor. Chem.* **2018**, *1139*, 44-49.
12. Yang, J. Q.; Gong, X. D.; Mei, H. Z.; Li, T.; Zhang, J. G.; Gozin, M. Design of Zero Oxygen Balance Energetic Materials on the Basis of Diels-Alder Chemistry. *J. Org. Chem.* **2018**, *83*, 14698-14702.
13. Wei, H.; Zhang, J. H.; He, C. L.; Shreeve, J. M.; Energetic Salts Based on

Furazan‐Functionalized Tetrazoles: Routes to Boost Energy. *Chem. Eur. J.* **2015**, *21*, 8607-8612.

14. Bennion, J. C.; Batyrev, I. G.; Ciezak-Jenkins, J. A.; High-Pressure Characterization of High-Performance Insensitive Energetic Materials: Dihydroxylammonium 5,5'-Bis(3-Nitro-1,2,4-Triazolate-1N-Oxide)(MAD-X1). *Propellants, Explos. Pyrotech.* **2019**, *44*, 160-165.
15. Gospodinov, I. V.; Hermann, Tobias.; Klapötke, T. M.; Stierstorfer, J. Energetic 8 Compounds Based on 3,4-Bis(4-nitramino-1,2,5-oxadiazol-3-yl)-1,2,5-furoxan 9 (BNAFF)[J]. *Propellants, Explos. Pyrotech.* **2018**, *43*, 355-363.
16. Wei, H.; Zhang, J. H.; He, C. L.; Shreeve, J. M. Combination of 1,2,4-Oxadiazole and 1,2,5-Oxadiazole Moieties for the Generation of High-Performance Energetic Materials. *Angew. Chem. Int. Ed.* **2015**, *54*, 9367-9371.
17. Pan, Y.; Zhu, W. H. Theoretical Design on A Series of Novel Bicyclic and Cage Nitramines as High Energy Density Compounds. *J. Phys. Chem. A* **2017**, *121*, 9163-9171.
18. He, P.; Zhang, J. G.; Wang, K.; Yin, X.; Jin, X.; Zhang, T. L. Extensive Theoretical Studies on Two New Members of the FOX-7 Family: 5-(Dinitromethylene)-1,4-Dinitramino-Tetrazole and 1,1'-Dinitro-4,'-Diamino-5,5'-Bitetrazole as Energetic Compounds. *Phys. Chem. Chem. Phys.* **2015**, *17*, 5840-5848
19. Wu, Q.; Zhang, Z. W.; Kou, B.; Zhu, W. H.; A DFT study of the structure–property relationships of bistetrazole-based high-nitrogen energetic metal complexes. J. Mol. Model. **2018**, *24*,119.
20. Tsyshevsky, R. V.; Pagoria, P.; Kuklja, M. M. Computational Design of Novel Energetic Materials: Dinitro-bis-triazolo-tetrazine. *J. Phys. Chem. C*, **2015**, *119*, 8512-8521.
21. He, P.; Zhang, J. G.; Wu, L.; Wu, J. T.; Zhang, T. L. Computational Design and Screening of Promising Energetic Materials: Novel Azobis(tetrazoles) with Ten Catenated Nitrogen Atoms Chain. *J. Phys. Org. Chem.* **2017**, *30*, e3674.
22. Fei, T.; Du, Y.; He, C. L.; Pang, S. P. Theoretical Investigations on Azole-fused Tricyclic 1,2,3,4-Tetrazine-2-oxides. *RSC Adv.* **2018**, *8*, 27235-27245.
23. Lu, T.; Chen, F. Multiwfn: A Multifunctional Wavefunction Analyzer. *J. Comput. Chem.* **2012**, *33*, 580-592.

24. Rice, B. M.; Pai, S. V.; Hare, J. Predicting Heats of Formation of Energetic Materials Using Quantum Mechanical Calculations. *Combust. Flame* **1999**, *118*, 445-458.
25. Mezger, M. J.; Tindle, K. J.; Pantoya, M.; Groven, L. J.; Kalyon, D. Energetic Materials: Advanced Processing Technologies for Next-generation Materials[M]. CRC Press, **2017**.
26. Pan, Y.; Zhu, W. H.; Xiao, H. M. Design and Selection of Nitrogen-rich Bridged Di-1,3,5-triazine Derivatives with High Energy and Reduced Sensitivity. *J. Mol. Model.* **2012**, *18*, 3125-3138.
27. Guo, Y. Y.; Chi, W. J.; Li, Z. S.; Li, Q. S. Molecular Design of N-NO_2 Substituted Cycloalkanes Derivatives $C_m(N\text{-}NO_2)_m$ for Energetic Materials with High Detonation Performance and Low Impact Sensitivity. *RSC Adv.* **2015**, *5*, 38048-38055.
28. Zhang, J. H.; Shreeve, J. M. Nitroaminofurazans with Azo and Azoxy Linkages: A Comparative Study of Structural, Electronic, Physicochemical, and Energetic Properties. *J. Phys. Chem. C* **2015**, *119*, 12887-12895.